

Endothelial dysfunction in ischemic acute renal failure: rescue by transplanted endothelial cells

SERGEY V. BRODSKY,^{1*} TOKUNORI YAMAMOTO,^{2*} TETSUHIRO TADA,³ BYUNGSOO KIM,¹ JUN CHEN,¹ FUMIHIKO KAJIYA,⁴ AND MICHAEL S. GOLIGORSKY¹

¹Departments of Medicine, Physiology, and Biophysics and Program in Bioengineering, State University of New York at Stony Brook, Stony Brook, New York 11794-8152; ²Departments of Urology and Medical Engineering, Kawasaki Medical School, Okayama 701-0114; and ³Department of Electrical Engineering, Okayama University of Science, and ⁴Department of Cardiovascular Physiology, Okayama University School of Medicine and Dentistry, Okayama 700-0005, Japan

Received 30 October 2001; accepted in final form 15 December 2001

Brodsky, Sergey V., Tokunori Yamamoto, Tetsuhiro Tada, Byungsoo Kim, Jun Chen, Fumihiko Kajiya, and Michael S. Goligorsky. Endothelial dysfunction in ischemic acute renal failure: rescue by transplanted endothelial cells. *Am J Physiol Renal Physiol* 282: F1140–F1149, 2002. First published December 18, 2001; 10.1152/ajprenal.00329.2001.—There is accumulating circumstantial evidence suggesting that endothelial cell dysfunction contributes to the “no-reflow” phenomenon in postischemic kidneys. Here, we demonstrated the vulnerability of in vitro, ex vivo, and in vivo endothelial cells exposed to pathophysiologically relevant insults, such as oxidative and nitrosative stress or ischemia. All of these stimuli compromised the integrity of the endothelial lining. Next, we performed minimally invasive intravital microscopy of blood flow in peritubular capillaries, which provided direct evidence of the existence of the no-reflow phenomenon, attributable, at least in part, to endothelial injury. In an attempt to ameliorate the hemodynamic consequences of lost endothelial integrity, we transplanted endothelial cells or surrogate cells expressing endothelial nitric oxide synthase into rats subjected to renal artery clamping. Implantation of endothelial cells or their surrogates expressing functional endothelial nitric oxide synthase in the renal microvasculature resulted in a dramatic functional protection of ischemic kidneys. These observations strongly suggest that endothelial cell dysfunction is the primary cause of the no-reflow phenomenon, which, when ameliorated, results in prevention of renal injury seen in acute renal failure.

endothelial cell transplantation; renal ischemia; intravital videomicroscopy; erythrocyte velocity; peritubular capillaries

THE PATHOPHYSIOLOGY OF ACUTE renal failure (ARF) has been tightly linked to tubular epithelial cell injury. In fact, most theories are based on this pathological feature, i.e., back-leakage, tubular obstruction, calcium overload, loss of cytoskeletal integrity, and loss of cell-matrix adhesion, all consider tubular epithelial cells as the main culprit (1, 17, 19, 29, 30, 34, 35, 37, 40, 41, 46,

52). Ischemic or nephrotoxic insults are believed to target principally and primarily the epithelium of the tubules, relegating to the endothelium a functional role in maintaining vasoconstriction (5).

However, three decades ago, Flores et al. (13) demonstrated that endothelial cells in the renal vasculature undergo an early swelling, leading to the narrowing of the lumen, an observation conceptualized in the “no-reflow” hypothesis (23, 43). This hypothesis has been supported by the observation that ischemic renal vasculature is characterized by a profound loss of acetylcholine-induced vasorelaxation (25). Conger et al. (7, 8) have demonstrated that vasorelaxation in response to stimuli generating endothelium-derived relaxing factor was inhibited in ARF. In addition, nitric oxide (NO) production in response to bradykinin was found to be suppressed in ischemic kidneys (33). Overexpression of intracellular adhesion molecule-1 (ICAM-1) by the vascular endothelium of the ischemic kidney has been demonstrated to play a major pathophysiological role in the development of renal dysfunction, and neutralizing anti-ICAM-1 antibodies significantly improved the outcome of renal ischemia (21). Furthermore, we have previously demonstrated that the endothelium of renal microvessels in ischemic kidneys show a loss of polarity in the expression of Arg-Gly-Asp-binding integrins, similar to that seen in the tubular epithelium (39). Most recently, permanent damage to peritubular capillaries has been discovered in rats subjected to renal ischemia (2). Collectively, these observations may be indicative of endothelial cell activation and dysfunction in ARF. If so, it becomes important to examine whether endothelial cell dysfunction is a cause of the tubular epithelial cell injury, its consequence, or an independent variable not affecting the course of ARF.

Here, we demonstrated the vulnerability of in vitro, ex vivo, and in vivo endothelial cells exposed to patho-

*S. V. Brodsky and T. Yamamoto contributed equally to this study. Address for reprint requests and other correspondence: M. S. Goligorsky, Dept. of Medicine, New York Medical College, Valhalla, NY 10595 (E-mail: Michael_Goligorsky@NYMC.edu).

The costs of publication of this article were defrayed in part by the payment of page charges. The article must therefore be hereby marked “advertisement” in accordance with 18 U.S.C. Section 1734 solely to indicate this fact.

physiologically relevant insults, such as oxidative and nitrosative stress, or to ischemia. These stimuli distorted the integrity of endothelial layers by desquamating or retracting cells. Next, we performed minimally invasive intravital microscopy of blood flow in peritubular capillaries, which directly demonstrated the existence of the no-reflow phenomenon. Finally, we showed that injection of endothelial cells or surrogate cells expressing endothelial NO synthase into rats subjected to renal artery clamping resulted in the implantation of these cells in the renal microvasculature. This was associated with a dramatic functional protection of ischemic kidneys. These observations strongly suggest that endothelial cell dysfunction is the primary cause of the no-reflow phenomenon, which, when ameliorated, results in prevention of tubular epithelial cell injury seen in ARF.

MATERIALS AND METHODS

Cell culture. Human umbilical vein endothelial cells (HUVEC) were obtained from Clonetics and maintained in EBM-2 medium under conditions of 37°C and 95% air-5% CO₂. HUVEC were used between passages 3 and 5. Before injection, cells were loaded with CellTracker (Molecular Probes) according to the manufacturer's protocol. Briefly, confluent HUVEC were lifted with trypsin-EDTA and suspended in EBM-2 medium. CellTracker was added (10 μM), and cells were incubated for 5 min at 37°C and then for an additional 15 min at 4°C. Wild-type and human embryonic kidney cells (HEK-293) stably expressing human endothelial NO synthase (eNOS), established by Liu et al. (26), were kindly provided by Dr. S. S. Gross (Cornell Medical College).

After being washed with PBS, cells were resuspended in EBM-2 (serum and growth factor free) at a final concentration of 5×10^6 cell/ml. The cell suspension was kept on ice until transplantation, but not longer than 30 min. Before injection, a small volume (5 μl) of cell suspension was aliquoted and replated on 35-mm dishes, and cell viability was tested 2 h later: >90% of cells excluded trypan blue. Simultaneously, fluorescence images of labeled cells were obtained to confirm the completeness of cell labeling.

Surgical procedure. All experiments were conducted in accordance with the *Guide for the Care and Use of Laboratory Animals* (National Research Council, 1996) and approved by the Institutional Animal Care and Use Committee. Male athymic nude rats weighing 160–180 g were allowed food and water ad libitum for 2 wk of recovery after transportation. After an overnight fast, animals were anesthetized with a combination of ketamine hydrochloride (6.0 mg/100 g) and xylazine hydrochloride (0.77 mg/100 g). The animals were placed on a heated surgical pad, and rectal temperature was maintained at 37°C. A subcutaneous injection of 250 units/kg heparin was given 15 min before the operation. A 2.5-cm midlaparotomy was performed, the right kidney was exposed, and two 3-0 sutures were passed under the renal pedicle in all rats. The left kidney was exposed, the renal artery was separated from the renal vein, and underpassed with a 3-0 suture. Renal ischemia (ischemic group) was initiated by clamping the left renal artery with microserrines (Fine Science Tools, Forster City, CA). After 45 min, the left renal artery was released, while the right renal pedicle and the right ureter were ligated, and a right nephrectomy was performed. After release of the clamp, 10⁶/0.2 ml HUVEC labeled with CellTracker (Molecular Probes) were injected into the right jugular vein or the aorta (through a

catheter inserted into the left carotid artery). The incision was closed with a 3-0 suture and surgical staples. Blood was drawn for determination of plasma creatinine concentration, using a Raichem kit (San Diego, CA) before and 24 h after the surgery. Sham-operated rats (right nephrectomy only) receiving intra-aortic infusion of the same dose of HUVEC served as controls. Tissue specimens (kidney, lung, liver, and spleen) were collected 24 h after clamp release for fluorescence and histochemical analyses. The scoring of renal injury was performed in a blinded fashion, as previously described (33).

Intravital microscopy and analysis of peritubular blood flow. Experiments were performed in animals surgically prepared as described above. Renal cortical peritubular capillaries were visualized by using a charge-coupled device video-microscope, with a pencil-lens probe having a tip diameter of 1 mm. The probe has a magnification of $\times 520$ and spatial resolution of 0.86 μm, permitting identification of individual erythrocytes (53, 54). Peritubular capillary blood flow was recorded on digital videocassette tapes before and after renal artery clamping. After 45-min renal artery occlusion, the clamp was removed, and reflow was initiated. The consecutive images of blood flow were collected at a rate of 30 frames/s for 60 min and at 24 h postoperatively. Images were analyzed using the freeze-frame mode. The velocity of red blood cells in individual segments of the peritubular capillaries was analyzed using a point-tracking method and motion-detection program (see Fig. 3C) written specifically for the study of peritubular capillary blood flow.

Cell detachment assay. HUVEC were cultured in 35-mm culture dishes. After cells were washed with PBS, 2 ml of Krebs-HEPES buffer with or without H₂O₂ or peroxyntirite, at final concentrations of 50 μM each, were added to each dish. Cells were incubated at room temperature on a Spec-Mix rocker shaker (Thermolyne, IA) at 12 rocks/min, 30° incline, and 10-μl aliquots were collected at specified times. The number of detached cells was counted using a Levy-Hausser counting chamber (Electron Microscopy Sciences). All experiments were repeated three times.

Histochemical techniques and scanning electron microscopy. Silver nitrate staining of endothelial cells was performed according to the previously described technique (12, 28). Briefly, anesthetized rats were perfused (through a catheter inserted into the left carotid artery) with 350 ml of fixative [1% paraformaldehyde and 0.5% glutaraldehyde in 75 mmol/l of cacodylate buffer (pH 7.4)] at a pressure of 120–140 mmHg for 5 min, followed by 80 ml of 0.9% NaCl for 2 min, 25 ml of 5% glucose for 10 s, 20 ml of 0.2% silver nitrate for 7 s, 25 ml of 5% glucose for 10 s, and 50 ml of fixative for 1 min.

After perfusion, the kidneys were removed, postfixed, and sectioned (30 μm thickness) using M-1 embedding matrix for frozen sections (LiPSHAW, Pittsburgh, PA). The silver halide was developed by a 15-min exposure to light emitted by a 150-W bulb. Finally, the kidney sections were dehydrated in alcohol, cleared in toluene, mounted in Permount, and observed with a Nikon Diaphot microscope. For counting of implanted CellTracker-labeled cells, HUVEC or HEK, kidneys were analyzed using confocal microscopy (Odyssey) with a 2-μm distance between consecutive focal planes. The number of cells in 50 separate areas was calculated for each group. Scanning electron microscopy was carried out on critical point-dried cells, as previously described (18).

Statistical analysis. Statistical analysis was performed using a paired or unpaired *t*-test and/or ANOVA followed by Tukey's posttest, with *P* < 0.05 considered significant. Comparison of the renal injury score among different groups was

carried out using nonparametric Kolmogorov-Smirnov analysis. Correlation analysis among the parameters of cell implantation, renal injury score, and plasma creatinine concentration was performed using nonparametric Spearman's correlation.

RESULTS

Oxidative and nitrosative stress impair the integrity of endothelial layers in vitro and in vivo. Confluent HUVEC were exposed to hydrogen peroxide (50 μ M) or peroxynitrite (50 μ M). Peroxynitrite resulted in a rapid detachment of endothelial cells (Fig. 1A), leading to the gradual loss of integrity of HUVEC monolayers. The latter was confirmed using scanning electron microscopy of endothelial monolayers subjected to peroxynitrite (50 μ M), which showed frequent gaps in its integrity (Fig. 1B). This finding is similar to that described by Nakamura et al. (31), who have observed a "peeling-off" phenomenon in endothelial cells subjected to the stimulated neutrophils or the neutrophil-derived oxidant NH_2Cl .

Perfusion of aortas ex vivo with Krebs buffer containing either 50 μ M hydrogen peroxide or 50 μ M peroxynitrite at a rate of 3 ml/min for 30 min resulted in the formation of gaps in the endothelial layer, as visualized using silver nitrite staining (not shown). In a series of in vivo experiments, silver nitrite staining of blood vessels obtained 4 h after release of the renal artery clamp showed that ischemic rats exhibited fre-

quent disorganization of endothelial integrity with areas of denudation, partial disappearance of cell-cell borders, or characteristic distortion of cell-cell contacts (Fig. 2). These defects in endothelial cell lining were most prominent in the renal microvasculature. The above in vitro and in vivo findings suggested the possibility that ischemia-reperfusion may compromise the barrier function of the endothelium in renal microvasculature.

Intravital microscopy of the blood flow in peritubular capillaries. Cortical blood flow in peritubular capillaries was visualized by intravital minimally invasive microscopy using a pencil-lens probe. In animals subjected to 45-min renal ischemia, the initially robust capillary blood flow partially recovered immediately after the release of the renal artery clamp, although many capillary loops remained nonperfused. However, within a minute blood flow again became stagnant for the next 3.6 ± 1.6 min ($n = 11$), after which time red blood cell velocity gradually recovered to approximately one-third of the initial speed. During this recovery process, many capillaries remained nonperfused for longer periods (Fig. 3a), probably explaining the characteristic patchiness of renal injury in acute renal ischemia. Recovery of the blood flow was nonlinear, displaying an oscillating pattern. During the recovery phase, the blood flow in individual capillaries exhibited both the orthograde and retrograde flow (not shown). Twenty-four hours after the release of the renal artery clamp, average red blood cell velocity in the peritubular capillaries was 227.5 ± 113 μ m/s (see also Fig. 7). These findings directly demonstrate the existence of a profound defect in the perfusion of peritubular capillaries of ischemic kidney.

In vivo injection of HUVEC improves renal function after renal artery cross-clamping. We argued that the loss of integrity of the endothelial layer, occurring in vivo after acute renal ischemia, may lead to the paradoxical vasoconstriction in response to endothelium-dependent vasorelaxing stimuli, similar to that observed by Furchgott and Zawadzki (14) in vascular segments with denuded endothelium. Given the possibility that the circulating endothelial cells may become implanted at the sites of endothelial denudation, athymic nude rats received a single injection of HUVEC (10^6 cells in 0.2 ml of serum-free culture medium) after a sham operation or after the release of the renal artery clamp. In rats that received 0.2 ml of a vehicle alone (serum-free cell culture medium), renal artery cross-clamping resulted in a significant elevation of plasma creatinine concentration (1.36 ± 0.2 vs. 0.38 ± 0.05 mg/dl in control, Fig. 4A). Intravenous infusion of HUVEC after the release of the renal artery clamp prevented the elevation of plasma creatinine concentration (0.66 ± 0.09 mg/dl, $P < 0.01$). The injection of HUVEC was also associated with a lesser degree of renal injury (Fig. 4B), scored in a blinded fashion, according to the previously described criteria (33). These data suggested that circulating exogenous endothelial cells could protect the kidney against ischemic injury.

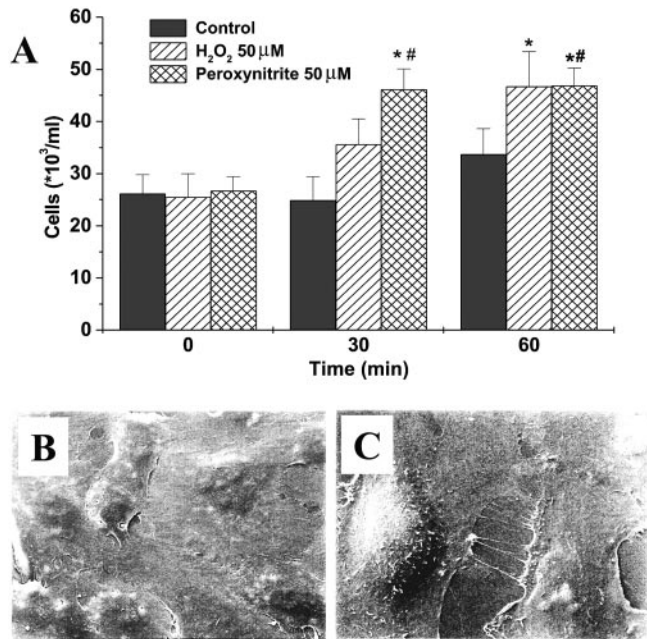


Fig. 1. Nitrosative and oxidative stress to cultured endothelial cells. A: no. of human umbilical vein endothelial cells (HUVEC) detached from the monolayer and recovered from the culture medium. Peroxynitrite results in a statistically significant increase in the no. of detached HUVEC within 30 min; hydrogen peroxide increases the number of detached HUVEC by 60 min of incubation. B and C: representative scanning electron microgram of the unstimulated HUVEC monolayer (B) and 30 min after stimulation with 50 μ M peroxynitrite. Formation of "gaps" between HUVEC is appreciable in C.

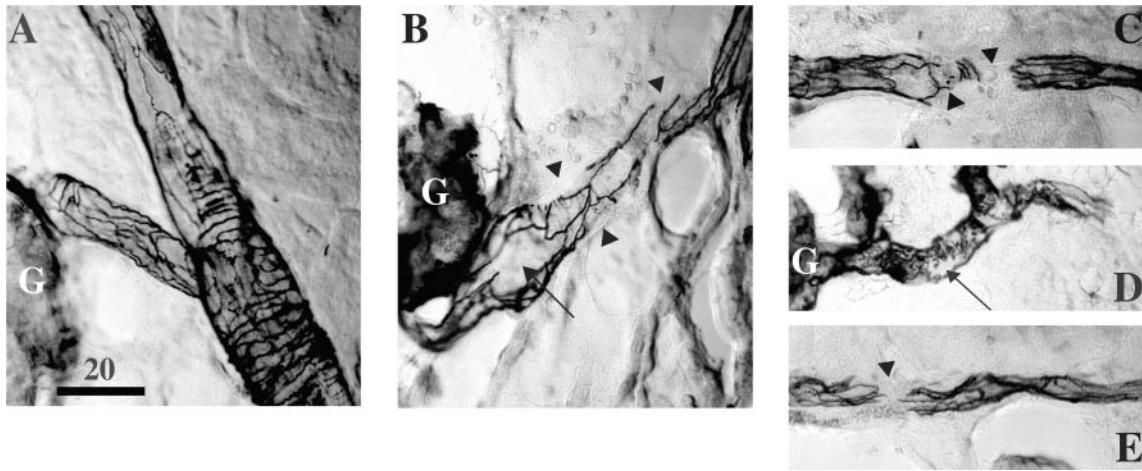


Fig. 2. Representative images of silver nitrite-stained afferent arterioles in control rats (A) and rats subjected to 45-min renal ischemia and 4-h reperfusion (B–E). Note that silver nitrite deposits at the perimeter of each endothelial cell in control microvessels, whereas in ischemic vessels areas of denudation (arrowheads) and partial loss of cell contours (arrows) are frequently observed. G, glomerulus. Bar = 20 μ m throughout.

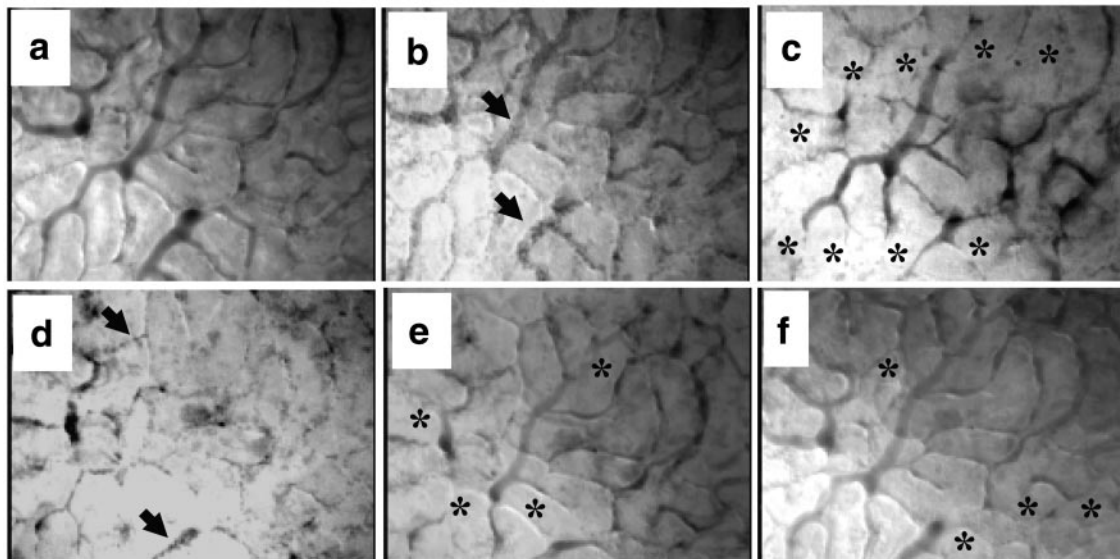
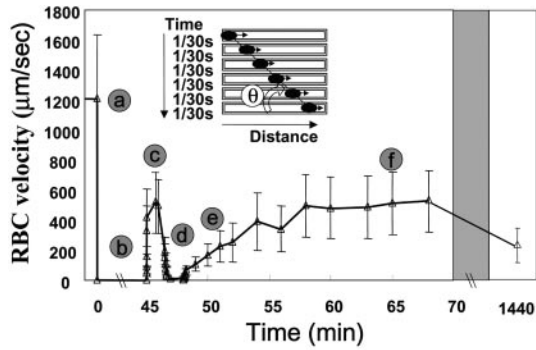


Fig. 3. Intravital imaging of the microcirculation in peritubular capillaries of postischemic kidneys. Erythrocyte velocity in peritubular capillaries (preischemic, ischemic, and postischemic values) is shown. *Inset*: schematic of the technique used to calculate erythrocyte velocity. Consecutive positions of the point-tracked erythrocyte provide the angle corresponding to its velocity. *a–f*: Consecutive images (*a–f* correspond to those in the *inset* and represent selected images obtained during videomicroscopy of postischemic kidneys at 0, 25, 46, 48, 50, and 65 min, respectively) of preischemic, ischemic, and postischemic peritubular capillaries. Note the blanching of the kidney and stagnant erythrocytes (arrows) during clamping of the renal artery and the second period of blanching and “no-reflow” during the reperfusion period. *, Nonperfused capillaries.

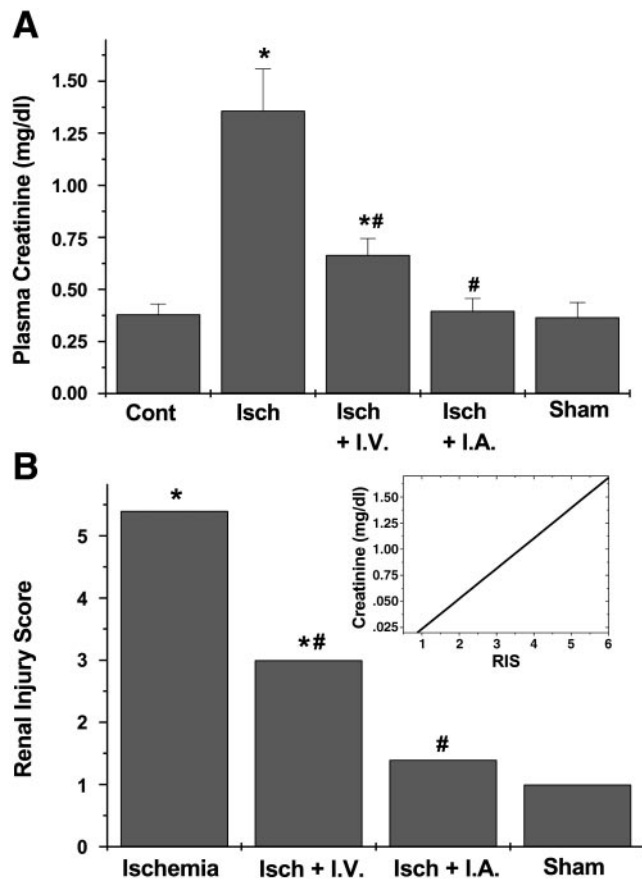


Fig. 4. Renal function and injury score in rats with renal ischemia receiving transplantation of HUVEC. A: plasma creatinine levels in control (Cont), sham-operated (Sham), and renal ischemia (Isch) animals receiving HUVEC via the intravenous (I.V.) or intra-aortic (I.A.) route. *Significantly different from control ($P < 0.05$, $n = 5$ rats/group). #Significantly different from ischemic group ($P < 0.05$, $n = 5$ rats/group). B: renal injury score in the same groups of animals. Statistical comparison between the groups was performed using a nonparametric Kolmogorov-Smirnov analysis. Inset: regression analysis of correlation between renal injury score (RIS) and plasma creatinine level. *Significantly different from control ($P < 0.05$, $n = 5$ rats/group). #Significantly different from ischemic group ($P < 0.05$, $n = 5$ rats/group).

To understand whether this effect required implantation of HUVEC in the renal vasculature, quantitative analysis of tissue cryosections was performed using fluorescence microscopy. The number of implanted HUVEC in different vascular beds (pulmonary, hepatic, splenic, renal glomeruli, peritubular capillaries, and vasa recta) was counted in 50 visual fields in each preparation ($n = 5$ rats each). The data presented in Fig. 5A show that the intravenous injection of HUVEC into sham-operated animals did not result in the preferential implantation of the labeled cells to any specific vascular bed, except for the higher number of implanted cells in the pulmonary circulation. In contrast, intravenous injection of labeled HUVEC into rats with ischemic renal failure led to the increased rates of implantation in renal and pulmonary vessels, with no significant increase in the number of HUVEC implanted in the splenic and hepatic vessels.

On the basis of the finding of significant entrapment of intravenously injected HUVEC in the pulmonary circulation, intra-aortic (via the carotid artery) injection of HUVEC was used in the next series of experiments. Determination of plasma creatinine concentration 24 h postischemia in this group of animals showed no significant differences from sham-operated rats (0.40 ± 0.06 mg/dl, $P < 0.001$). Renal injury in this group was largely prevented (Fig. 4B). Analysis of implantation of HUVEC in different vascular beds demonstrated that, with intra-aortic injection, the renal vasculature showed preferential implantation of the injected cells. Labeled HUVEC (CellTracker) implanted in higher density in glomeruli, peritubular capillaries, and vasa recta of ischemic, compared with sham-operated, kidneys (Figs. 5, A and B, and 6).

There was a strong correlation between plasma creatinine and the degree of renal injury (Spearman's correlation coefficient, $r = 0.91$, $P = 0.042$) (Fig. 4, inset) and between plasma creatinine vs. the number of

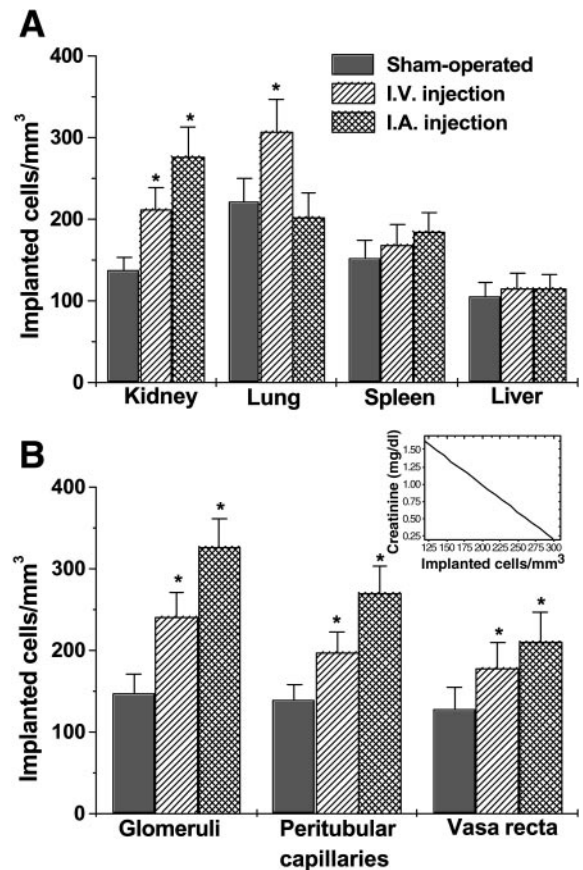


Fig. 5. Extrarenal and renal distribution of transplanted HUVEC. A: density of implanted HUVEC. Before transplantation, HUVEC were labeled with CellTracker and injected as detailed in MATERIALS AND METHODS. Frozen sections were obtained from different organs and examined under a fluorescence microscope. Note the entrapment of HUVEC in the pulmonary circulation after intravenous injection and the high no. of implanted HUVEC in the renal microcirculation after intra-aortic injection. B: distribution of implanted HUVEC within the renal microcirculation. Inset: regression analysis of correlation between no. of implanted cells and plasma creatinine level. * $P < 0.05$ vs. sham-operated control.

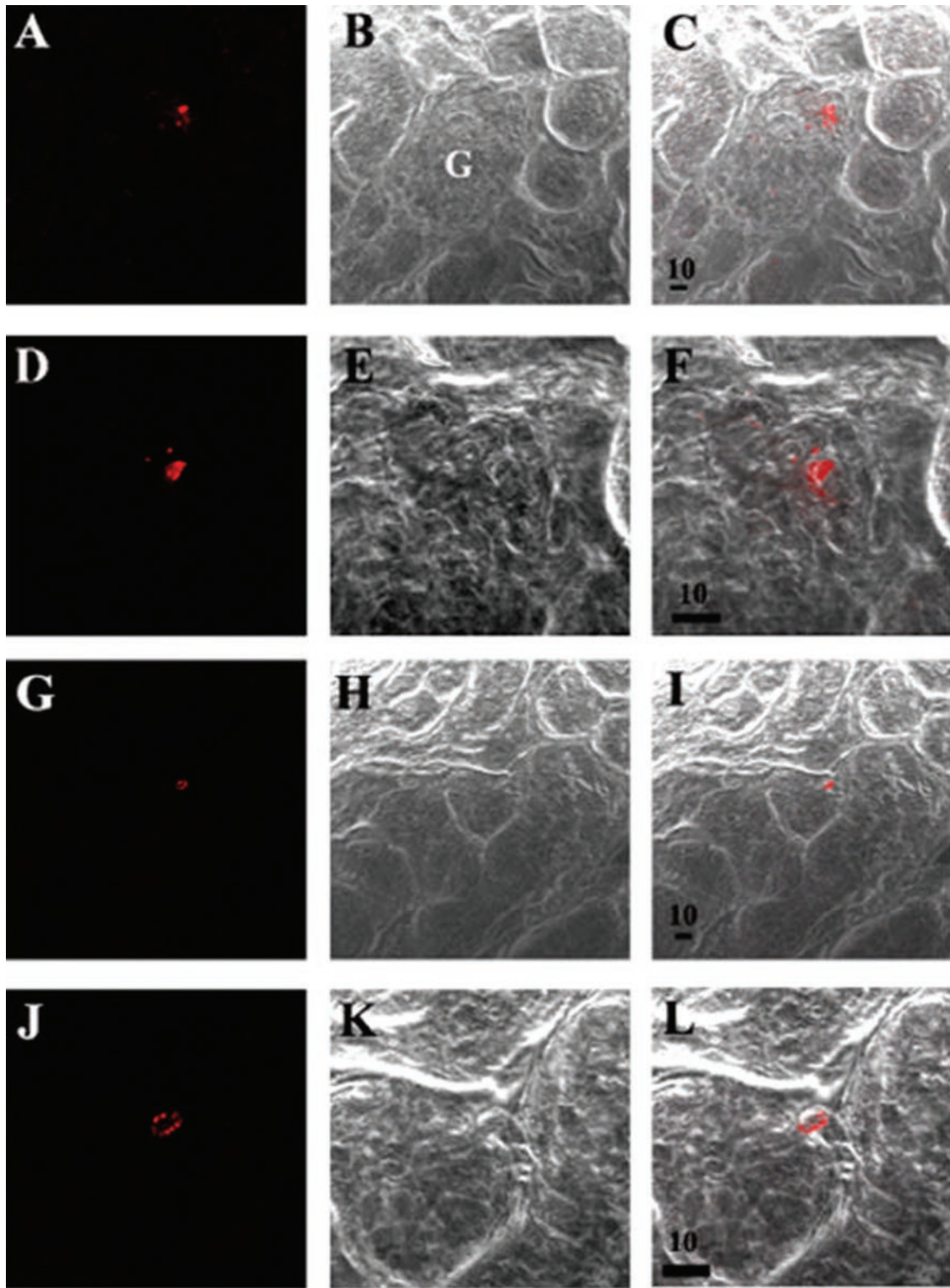


Fig. 6. Representative combined confocal fluorescence and brightfield microscopy images of a glomerular (A–F) and peritubular capillaries (G–L). A, D, G, and J: fluorescence microscopy. B, E, H, and K: brightfield frames of the same images. C, F, I, and L: merged fluorescence and brightfield images. D–F and J–L: higher magnification of images shown in A–C and G–I, respectively, demonstrating fluorescently tagged implanted endothelial cells.

implanted endothelial cells ($r = -0.85$, $P = 0.008$) (Fig. 5, *inset*). The correlation between the number of implanted endothelial cells and the degree of renal injury ($r = -0.64$, $P = 0.069$) did not reach statistical significance. Nonetheless, correlation analysis demonstrated a clear-cut connection between the density of implanted endothelial cells and the functional outcome of acute renal ischemia.

In vivo injection of HEK cells stably expressing human eNOS improves renal function after renal artery cross-clamping. To elucidate the functional role of defective eNOS generation of NO (23) and its improvement by implantation of intact endothelial cells, in the next series of experiments we utilized HEK cells stably expressing human eNOS (HEK/eNOS) as surrogates for endothelial cells. In vivo intra-aortic infusion of HEK/eNOS cells after release of the renal artery clamp

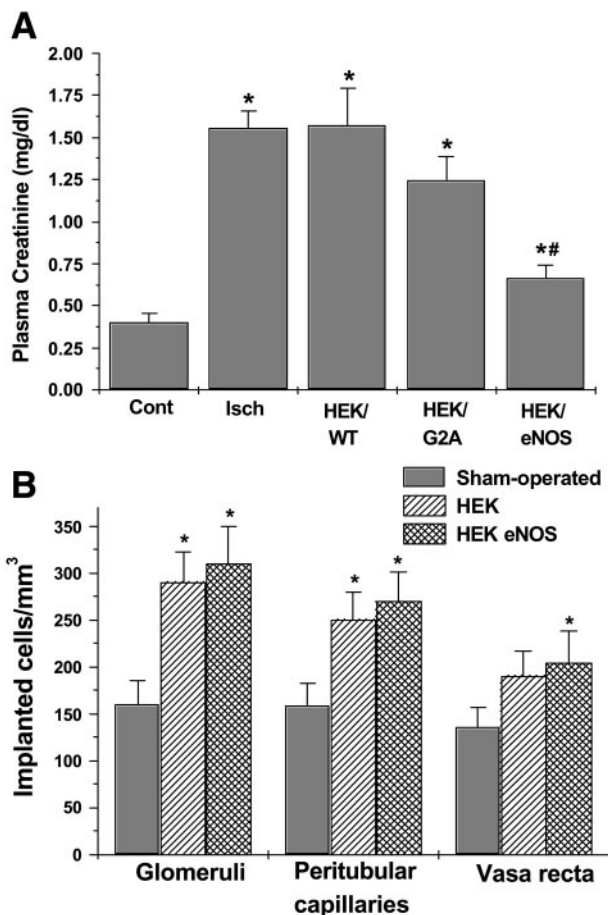


Fig. 7. Renal function in rats subjected to renal ischemia and transplanted with human embryonic kidney (HEK) cells. **A:** HEK cells, either wild-type (WT) or those stably expressing a palmitoylation-deficient (HEK/G2A) or wild-type human endothelial nitric oxide synthase [HEK/endothelial nitric oxide synthase (eNOS)], were injected intra-arterially after the release of renal artery clamp. Creatinine concentration 24 h postischemia showed a significant reduction in animals receiving HEK/eNOS cell transplantation. *Significantly different from control (Cont; $P < 0.05$, $n = 5$ rats/group). #Significantly different from ischemic group (Isch; $P < 0.05$, $n = 5$ rats/group). **B:** distribution of implanted wild-type or eNOS-expressing HEK cells within renal microvasculature ($P < 0.05$, $n = 5$ rats/group). * $P < 0.05$ vs. sham-operated control.

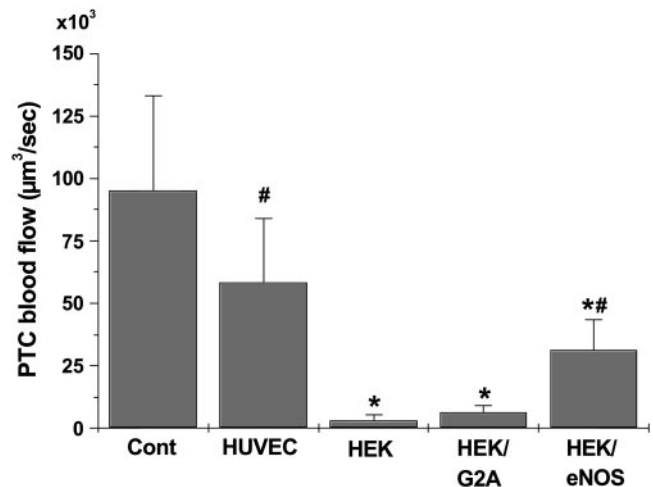


Fig. 8. Blood flow in peritubular capillaries of rats subjected to renal ischemia and treated with transplantation of HUVEC or HEK cells. Twenty-four hours postischemia, blood flow in peritubular capillaries (PTC) was measured using intravital videomicroscopy, as detailed in MATERIALS AND METHODS. # $P < 0.05$ vs. control. * $P < 0.05$ vs. HUVEC-injected group.

resulted in the amelioration of renal dysfunction (Fig. 7A). In contrast, wild-type HEK cells, devoid of eNOS, did not affect the degree of renal dysfunction 24 h postischemia. Similar results were obtained in rats injected with HEK cells stably expressing the palmitoylation-deficient eNOS (HEK/G2A), which has been previously demonstrated to abolish the ability to produce NO (26). Despite these functional differences, the density of implantation of wild-type and eNOS-expressing HEK cells was not significantly different in ischemic kidneys and was again significantly lower in kidneys from sham-operated animals (Fig. 7B).

Intravital videomicroscopy and measurement of red blood cell velocity in peritubular capillaries showed that HUVEC-injected kidneys (Fig. 8) displayed significant hemodynamic improvement. Microcirculatory hemodynamics were not affected by the transplantation of HEK or HEK/G2A cells. In contrast, HEK/eNOS cells afforded significant hemodynamic protection to the ischemic kidneys.

DISCUSSION

The data presented herein demonstrate the vulnerability of endothelial cells to nitrosative and oxidative stress in vitro and renal artery cross-clamping in vivo, suggesting that the vascular endothelium may represent one of the targets in renal ischemia. Furthermore, animals injected with a suspension of intact endothelial cells showed that these cells implanted in the renal microvasculature, a phenomenon which was associated with the improved renal function. These data lend support to the idea that endothelial cell dysfunction represents a proximal pathophysiological trigger for ensuing epithelial cell damage in acute renal ischemia.

The previous paradoxical observation that nonselective NOS inhibitors exaggerate renal damage after renal artery clamping, whereas selective inhibition of

inducible NOS (iNOS) protected renal function against ischemia, alluded to the critical role of endothelial function in determining the outcome of renal ischemia (33). Together with the demonstration of reduced NO production by ischemic kidneys stimulated with bradykinin (33), these findings implicated eNOS as an important contributor to the loss of kidney function after renal artery cross-clamping.

It has been demonstrated that tissue ischemia and cytokines mobilize bone marrow-derived endothelial progenitor cells (45) and that circulating endothelial cells of hematopoietic origin are recruited to ischemic areas to form adult blood vessels (10). Hence, one may argue that the observed amelioration of renal dysfunction after renal artery clamping could be explained by the above mechanism. Both processes, however, occur on a time scale of 3–7 days to several weeks, respectively, thus effectively precluding *de novo* angiogenic mechanisms as major contributors to the observed dramatic improvement in postischemic renal function. We therefore concluded that pathophysiologically relevant events should take place in the early postischemic period. This conclusion was further supported by the previous observation of Bird et al. (3) indicating successful amelioration of renal ischemic injury on improvement of microcirculation using the antioxidant probucol.

Minimally invasive intravital microscopy of peritubular capillary blood flow in control and postischemic kidneys provided the direct characterization of renal microvascular hemodynamics and confirmed the existence of the no-reflow phenomenon. This was characterized by a sudden cessation of the peritubular capillary flow within 1–3 min after the removal of the clamp, followed by a gradual and partial recovery of the microcirculatory blood flow. During the recovery process, restoration of blood flow was not uniform but rather sporadic capillaries showed stagnation or cessation of flow. Twenty-four hours postischemia, blood flow in the peritubular capillaries remained severely impaired in nontreated or vehicle-treated animals but improved significantly in animals transplanted with HUVEC and HEK/eNOS. The question arises, Is NO generated by a relatively small number of engrafted cells sufficient for improving renal microcirculation? The observed chaotic distribution of endothelial injury and/or denudation scattered in renal microvasculature is in concert with the apparently chaotic involvement of peritubular capillaries in no-reflow. Assuming that a significant proportion of transplanted cells engraft in the areas of denudation, it is possible that, by preventing no-reflow at these scattered sites, even a relatively small number of engrafted NO-producing cells could improve microcirculation.

The salient finding that endothelial cells can rescue the function of an ischemic organ consisting of different cell types illustrates a more general principle of cell-cell interaction, in which the dysfunction of one cell type affects the functions of other cells. For instance, abdominal radiation injury, known to produce severe diarrhea and damage to the crypts of Lieberkuhn, was

previously attributed to the lethal damage of epithelial stem cells. However, recent evidence indicates that the primary lesion in intestinal radiation syndrome occurs in microvascular endothelial cells (36). Epithelial cell exfoliation triggered by abnormalities in the vasculature have been shown in the gastric mucosa. Injury to the gastric microvasculature or severe vasoconstriction induced by endothelin-1 caused an almost complete exfoliation of the interpit cells and apoptosis of superficial cells of gastric mucosa, with the eventual formation of ulcers (42). Exposing gastric mucosa to aspirin resulted in exfoliation of surface epithelium and deep mucosal necrosis, which was preceded by microvascular injury manifesting itself as the rupture of capillary walls, necrosis of the endothelium, deposition of fibrin, and platelet adhesion (47). Similar findings were reported after intragastric administration of ethanol in healthy volunteers (48). Together with our findings, these data may allude to a more general principle: endothelial dysfunction leads to injury of nonendothelial cells located within the basin of a feeding capillary.

Therapeutic strategies based on the use of endothelial progenitor cells have been described. In rats with acute myocardial ischemia induced by ligation of the left anterior descending coronary artery, transplantation of endothelial progenitor cells partially rescued left ventricular function (20). This effect was attributed to improved angiogenesis in the ischemic myocardium, although the possible role of improved vascular function was not addressed in the study. In diabetic mice, but not in control animals, transplantation of blood-derived angioblasts accelerated the restoration of blood flow to an ischemic hindlimb (40). This differential response in diabetic and control animals may be related to the preexisting endothelial dysfunction in animals that benefited from angioblast transplantation (reviewed in Ref. 5). However, in acute renal ischemia, we reasoned that the use of endothelial progenitor cells did not appear to represent the strategy of choice due to the protracted period of differentiation of transplanted cells (10, 45) and gave preference to the use of fully differentiated HUVEC for transplantation.

Recently accumulated evidence suggests that many aspects of endothelial dysfunction are intimately linked to the expression and function of eNOS and/or bioavailability of NO (27). In particular, NO generation inhibits platelet aggregation and adhesion of leukocytes to the vascular endothelium (11, 22, 24, 32, 44, 49). Endothelial regulation of vascular smooth muscle relaxation, proliferation, and migration is, in part, governed by the integrity of the L-arginine-eNOS-NO system (15, 38, 51). In addition, vascular/endothelial permeability and some synthetic functions of endothelial cells have been linked to the activity of eNOS (reviewed in Ref. 6). Hence, NO production or availability can regulate diverse functions in endothelial cells *per se* and their interaction with circulating formed elements (both inflammatory and thrombogenic interactions) and vascular smooth muscle cells. Despite the fact that NO generation in epithelia of ischemic kidneys is excessive due to the induction of iNOS, endothelial gen-

eration of NO appears to be compromised (33), thus participating in the pathogenesis of no-reflow. The previous suggestion that the lack of endothelium-dependent vasorelaxation in postischemic kidneys is due to the maximal stimulation of eNOS (9), mainly on the basis of the increased expression of eNOS 1 wk after ischemic insult, perhaps reflects on "uncoupled" eNOS generating superoxide but has no direct relevance to the present findings.

On the basis of these considerations, we performed an additional series of experiments utilizing HEK cells stably expressing eNOS or its palmitoylation-deficient mutant. The results of these experiments demonstrated that the implantation of cells expressing the functional eNOS, not necessarily endothelial cells per se, was sufficient to ameliorate renal dysfunction accompanying acute ischemia. These findings further implicate eNOS and endothelial cell dysfunction in the initiation of pathophysiological cascades leading to ischemic ARF.

The studies presented herein were not designed to define a therapeutic approach to prevention of ARF with injected endothelial cells. Rather, they provide a proof of the principle that endothelial cell dysfunction triggers the pathophysiological cascade of events resulting in ischemic renal injury. Endothelial cell dysfunction should be seen in a broader context of the "fight-or-flight" cellular reaction to stress (16). This reaction has been proposed to serve as a default mechanism, leading to cell detachment under stress situations. Therefore, it is possible that endothelial cell dysfunction is not an isolated feature of ischemic acute renal injury but may be a companion of renal injury initiated by other etiological factors.

The authors are grateful to Dr. Leon Moore (Dept. of Physiology, SUNY Stony Brook) for critically reading the manuscript.

These studies were supported in part by National Institute of Diabetes and Digestive and Kidney Diseases Grants DK-45462, DK-54602, and DK-52783 (M. S. Goligorsky), American Heart Association Fellowship 0120200T (S. V. Brodsky), and sabbatical support from the Catholic University of Seoul, South Korea (B. Kim).

REFERENCES

1. **Arendshorst W, Finn W, and Gottschalk CW.** Micropuncture study of acute renal failure following temporary renal ischemia in the rat. *Kidney Int Suppl* 6: S100–S105, 1976.
2. **Basile DP, Donohoe D, Roethe K, and Osborn JL.** Renal ischemic injury results in permanent damage to peritubular capillaries and influences long-term function. *Am J Physiol Renal Physiol* 281: F887–F899, 2001.
3. **Bird JE, Evan A, Peterson O, and Blantz RC.** Early events in ischemic renal failure in the rat: effects of antioxidant therapy. *Kidney Int* 35: 1282–1289, 1989.
4. **Brady H, Brenner B, and Lieberthal W.** Acute renal failure. In: *The Kidney*, edited by Brenner B. Philadelphia, PA: Saunders, 1996, p. 1200–1252.
5. **Calles-Escandon J and Cipolla M.** Diabetes and endothelial dysfunction: a clinical perspective. *Endocr Rev* 22: 36–52, 2001.
6. **Cines DB, Pollak ES, Buck CA, Loscalzo J, Zimmerman GA, McEver RP, Pober JS, Wick TM, Konkle BA, Schwartz BS, Barnathan ES, McCrae KR, Hug BA, Schmidt AM, and Stern DM.** Endothelial cell in physiology, and in the pathophysiology of vascular disorders. *Blood* 91: 3527–3561, 1998.
7. **Conger JD, Robinette J, and Guggenheim S.** Effect of acetylcholine on the early phase of norepinephrine-induced acute renal failure. *Kidney Int* 19: 399–409, 1981.
8. **Conger JD, Robinette J, and Schrier RW.** Smooth muscle calcium and endothelium-derived relaxing factor in the abnormal vascular responses of acute renal failure. *J Clin Invest* 82: 532–537, 1988.
9. **Conger J, Robinette J, Villar A, Raij L, and Shultz P.** Increased nitric oxide synthase activity despite lack of response to endothelium-dependent vasodilators in postischemic acute renal failure in rats. *J Clin Invest* 96: 631–638, 1995.
10. **Crosby J, Kaminski W, Schattman G, Martin P, Raine E, Seifert R, and Bowen-Pope DF.** Endothelial cells of hematopoietic origin make a significant contribution to adult blood vessel formation. *Circ Res* 87: 728–730, 2000.
11. **De Caterina R, Libby P, Peng H, Thannickal V, Rajaveshth T, Gimbrone M, Shin W, and Liao J.** Nitric oxide decreases cytokine-induced endothelial activation. *J Clin Invest* 96: 60–68, 1995.
12. **Ezaki T, Baluk P, Thurston G, La Barbara A, Woo C, and McDonald DM.** Time course of endothelial cell proliferation and microvascular remodeling in chronic inflammation. *Am J Pathol* 158: 2043–2055, 2001.
13. **Flores J, DiBona D, Beck C, and Leaf A.** The role of cell swelling in ischemic renal damage and the protective effect of hypertonic solute. *J Clin Invest* 51: 118–126, 1972.
14. **Furchgott RF and Zawadzki JW.** The obligatory role of endothelial cells in the relaxation of arterial smooth muscle by acetylcholine. *Nature* 288: 373–376, 1980.
15. **Garg UC and Hassid A.** Nitric oxide-generating vasodilators and 8-bromo-cyclic guanosine monophosphate inhibit mitogenesis and proliferation of cultured rat vascular smooth muscle cells. *J Clin Invest* 83: 1774–1777, 1989.
16. **Goligorsky MS.** The concept of cellular "fight-or-flight" reaction to stress. *Am J Physiol Renal Physiol* 280: F551–F561, 2001.
17. **Goligorsky M and DiBona GF.** Pathogenetic role of Arg-Gly-Asp-recognizing integrins in acute renal failure. *Proc Natl Acad Sci USA* 90: 5700–5705, 1993.
18. **Goligorsky MS, Menton D, Laszlo A, and Lum H.** Nature of thrombin-induced sustained elevation in cytosolic calcium concentration in cultured endothelial cells. *J Biol Chem* 264: 16771–16775, 1989.
19. **Heyman SN, Brezis M, Reubinoff CA, Greenfeld Z, Lechene C, Epstein FH, and Rosen S.** Acute renal failure with selective medullary injury in the rat. *J Clin Invest* 82: 401–412, 1988.
20. **Kawamoto A, Gwon HC, Iwaguro H, Yamaguchi JI, Uchida S, Masuda H, Silver M, Ma H, Kearney M, Isner JM, and Asahara T.** Therapeutic potential of ex vivo expanded endothelial progenitor cells for myocardial ischemia. *Circulation* 103: 634–637, 2001.
21. **Kelly K, Williams W, Colvin B, and Bonventre JV.** Antibody to intercellular adhesion molecule-1 protects the kidney against ischemic injury. *Proc Natl Acad Sci USA* 91: 812–817, 1994.
22. **Kubes P, Suzuki M, and Granger DN.** Nitric oxide: an endogenous modulator of leukocyte adhesion. *Proc Natl Acad Sci USA* 88: 4651–4655, 1991.
23. **Leaf A.** Cell swelling: a factor in ischemic tissue injury. *Circulation* 48: 455–458, 1973.
24. **Leibovich SJ, Polverini PJ, Fong TW, Harlow LA, and Koch AE.** Production of angiogenic activity by human monocytes requires an L-arginine/nitric oxide-synthase-dependent effector mechanism. *Proc Natl Acad Sci USA* 91: 4190–4194, 1994.
25. **Lieberthal W, Wolf E, Rennke HG, Valeri CR, and Levinsky NG.** Renal ischemia and reperfusion impair endothelium-dependent vascular relaxation. *Am J Physiol Renal Fluid Electrolyte Physiol* 256: F894–F900, 1989.
26. **Liu J, Garcia-Cardena G, and Sessa WC.** Palmitoylation of endothelial nitric oxide synthase is necessary for optimal stimulated release of nitric oxide: implications for caveolar localization. *Biochemistry* 35: 13277–13281, 1996.

27. **Ludmer PL, Selwyn AP, Shook LT, Wayne RR, Mudge GH, Alexander RW, and Ganz P.** Paradoxical vasoconstriction induced by acetylcholine in atherosclerotic coronary arteries. *N Engl J Med* 315: 1046–1051, 1986.
28. **McDonald DM.** Endothelial gaps and permeability of venules in rat tracheas exposed to inflammatory stimuli. *Am J Physiol Lung Cell Mol Physiol* 266: L61–L83, 1994.
29. **Molitoris BA and Nelson WJ.** Alterations in the establishment and maintenance of epithelial cell polarity as a basis for disease processes. *J Clin Invest* 85: 3–9, 1990.
30. **Myers BD and Moran SM.** Hemodynamically mediated acute renal failure. *N Engl J Med* 314: 97–105, 1986.
31. **Nakamura TY, Yamamoto I, Nishitani H, Matozaki T, Suzuki T, Wakabayashi S, Shigekawa M, and Goshima K.** Detachment of cultured cells from the substratum induced by the neutrophil-derived oxidant NH₂Cl: synergistic role of phosphotyrosine and intracellular Ca²⁺ concentration. *J Cell Biol* 131: 509–524, 1995.
32. **Niu X, Smith CW, and Kubes P.** Intracellular oxidative stress induced by nitric oxide synthesis inhibition increases endothelial cell adhesion to neutrophils. *Circ Res* 74: 1133–1140, 1994.
33. **Noiri E, Peresleni T, Miller F, and Goligorsky MS.** Antisense oligonucleotides to the inducible NOS prevent tubular cell death in ischemic acute renal failure. *J Clin Invest* 97: 2377–2383, 1996.
34. **Oliver J.** Correlation of structure and function and mechanisms of recovery in acute tubular necrosis. *Am J Med* 15: 535–557, 1953.
35. **Oliver J, MacDowell M, and Tracy A.** The pathogenesis of acute renal failure associated with traumatic and toxic injury. Renal ischemia, nephrotoxic damage, and the ischemic episode. *J Clin Invest* 30: 1307–1351, 1951.
36. **Paris F, Fuks Z, Kang A, Capodiceci P, Juan G, Ehleiter D, Haimovitz-Friedman A, Cordon-Cardo C, and Kolesnick R.** Endothelial apoptosis as the primary lesion initiating intestinal radiation damage in mice. *Science* 293: 293–297, 2001.
37. **Reubi RC and Vorburger C.** Renal hemodynamics in acute renal failure after shock in man. *Kidney Int* 6: S137–S143, 1976.
38. **Reyes A, Porras B, Chasalow F, and Klahr S.** L-arginine decreases the infiltration of the kidney by macrophages in obstructive nephropathy and puromycin-induced nephrosis. *Kidney Int* 45: 1346–1354, 1994.
39. **Romanov V, Noiri E, Czerwinski G, Finsinger D, Kessler H, and Goligorsky MS.** Two novel probes reveal tubular and vascular RGD binding sites in the ischemic rat kidney. *Kidney Int* 52: 93–102, 1997.
40. **Schatteman G, Hanlon H, Jiao C, Dobbs S, and Christy B.** Blood-derived angioblasts accelerate blood-flow restoration in diabetic mice. *J Clin Invest* 106: 571–578, 2000.
41. **Schrier RW, Arnold P, Van Putten V, and Burke TJ.** Cellular calcium in ischemic acute renal failure: role of calcium entry blockers. *Kidney Int* 32: 313–321, 1987.
42. **Spyridon L, Akira N, Hiromasa K, Katsutoshi G, Takao M, Yoshiki O, Hideo S, and Hisayuki F.** The development of the endothelin-1-induced gastric ulcer: time sequence analysis of morphologic changes. *Int J Exp Pathol* 75: 345–355, 1994.
43. **Summers W and Jamison RL.** The no-reflow phenomenon in renal ischemia. *Lab Invest* 25: 635–643, 1971.
44. **Sundquist T, Forslund T, Bengtsson T, and Axelsson K.** S-nitroso-N-acetylpenicillamine reduces leukocyte adhesion to type I collagen. *Inflammation* 18: 625–631, 1994.
45. **Takahashi T, Kalka C, Masuda H, Chen D, Silver M, Kearney M, Magner M, Isner J, and Asahara T.** Ischemia- and cytokine-induced mobilization of bone marrow-derived endothelial progenitor cells for neovascularization. *Nature Med* 5: 434–438, 1999.
46. **Tanner GA and Steinhausen M.** Kidney pressure after temporary artery occlusion in the rat. *Am J Physiol* 230: 1173–1181, 1976.
47. **Tarnawski A, Stachura J, Gergely H, and Hollander D.** Gastric microvascular endothelium: a major target for aspirin-induced injury and arachidonic acid protection. An ultrastructural analysis in the rat. *Eur J Clin Invest* 20: 432–440, 1990.
48. **Tarnawski A, Stachura J, Gergely H, and Hollander D.** Microvascular endothelium: a major target for alcohol injury of the human gastric mucosa. Histochemical and ultrastructural study. *J Clin Gastroenterol* 10, Suppl 1: S53–S64, 1988.
49. **Thom S, Ohnishi T, and Ischiropoulos H.** Nitric oxide released by platelets inhibits neutrophil β2 integrin function following acute carbon monoxide poisoning. *Tox Appl Pharm* 128: 105–110, 1994.
50. **Venkatachalam MA, Jones D, Rennke HG, Sandstrom D, and Patel Y.** Mechanism of proximal tubule brush border loss and regeneration following mild ischemia. *Lab Invest* 45: 355–365, 1981.
51. **Von der Leyen H, Gibbons G, Morishita R, Lewis N, Zhang L, Nakajima M, Kaneda Y, Cooke J, and Dzau VJ.** Gene therapy inhibiting neointimal vascular lesion: in vivo transfer of endothelial cell nitric oxide synthase gene. *Proc Natl Acad Sci USA* 92: 1137–1141, 1995.
52. **Weinberg JM.** The cell biology of ischemic renal injury. *Kidney Int* 39: 476–500, 1991.
53. **Yamamoto T, Hayashi K, Matsuda H, Kubota E, Tanaka H, Ogasawara Y, Nakamoto H, Suzuki H, Saruta T, and Kajiya F.** In vivo visualization of angiotensin-II and TGF-mediated renal vasoconstriction. *Kidney Int* 60: 364–369, 2001.
54. **Yamamoto T, Tomura Y, Tanaka H, and Kajiya F.** In vivo visualization of renal microcirculation in hypertensive and diabetic rats. *Am J Physiol Renal Physiol* 281: F571–F577, 2001.